

Spatial-Stiffness Analysis of Surface-Based Registration

Burton Ma and Randy E. Ellis

School of Computing, Queen's University at Kingston, Canada K7L 3N6

Abstract. We have developed a new approach for preoperative selection of points from a surface model for rigid shape-based registration. This approach is based on an extension of our earlier spatial-stiffness model of fiducial registration. We compared our approach with the maximization of the noise-amplification index (NAI), using target registration accuracy (TRE) as our comparison measure, on models derived from computed tomography scans of volunteers. In this study, our approach was substantially less expensive to compute than maximizing the NAI and produced similar TREs with smaller variances. Optimal incremental selection shows promise for improving the preoperative selection of registration points for image-guided surgical procedures.

1 Introduction

A patient's anatomy can be registered to preoperative 3D medical images for use in image-guided surgery by digitizing anatomical registration points on the patient and matching them to surface models derived from the images. We propose a method for choosing model registration points from the preoperative medical image, based on an extension of the method we described in Ma and Ellis [5] for fiducial registration. We view the registration points as the points where an elastic suspension system is attached to a rigid mechanism. By analyzing the stiffness matrix of the mechanism using the techniques developed by Lin et al. [3], we are able to compute a stiffness-quality measure that characterizes the least constrained displacement of the mechanism with respect to a target. The analysis yields the direction of translation or the axis of rotation of the least constrained displacement. The form of the stiffness matrix suggests a way to add a new point to stiffen this displacement thereby improving the quality measure. An unresolved problem is how to relate these preoperative registration points to anatomical registration points derived from the patient.

2 Stiffness of a Passive Mechanical System

The background material, from the robotics literature, is mainly from Lin et al. [3] and is a condensed version of one from our previous work [5]. This material is also related to the compliant axes given by Patterson and Lipkin [9].

A general model of the elastic behavior of a passive unloaded mechanism is a rigid body that is suspended by linear and torsional springs, which leads to analysis of the spatial stiffness or compliance of the mechanism. For a passive mechanism in local equilibrium, a twist displacement \mathbf{t} of a rigid body is related to a counteracting wrench force \mathbf{w} by a 6×6 spatial stiffness matrix \mathbf{K} :

$$\mathbf{w} = \mathbf{K}\mathbf{t} = \begin{bmatrix} \mathbf{A} & \mathbf{B} \\ \mathbf{B}^T & \mathbf{D} \end{bmatrix} \mathbf{t} \quad (1)$$

where \mathbf{A} , \mathbf{B} , and \mathbf{D} are 3×3 matrices. The twist is a vector $\mathbf{t} = [\mathbf{v}^T \ \boldsymbol{\omega}^T]^T$ where $\mathbf{v}^T = [v_x \ v_y \ v_z]$ is linear displacement and $\boldsymbol{\omega}^T = [\omega_x \ \omega_y \ \omega_z]$ is rotational displacement. The wrench is a vector $\mathbf{w} = [\mathbf{f}^T \ \boldsymbol{\tau}^T]^T$ where $\mathbf{f}^T = [f_x \ f_y \ f_z]$ is force and $\boldsymbol{\tau}^T = [\tau_x \ \tau_y \ \tau_z]$ is torque. Equation 1 is simply a general, vectorial expression of Hooke's Law. We can obtain \mathbf{K} by evaluating the Hessian of the potential energy U of the system at equilibrium (Mishra and Silver [6]).

\mathbf{K} is a symmetric positive-definite matrix for stable springs and small displacements from equilibrium. The eigenvalues of \mathbf{K} are not immediately useful because their magnitudes change with the coordinate frame used to define \mathbf{K} ; however, it can be shown that the eigenvalues of

$$\mathbf{K}_V = \mathbf{D} - \mathbf{B}^T \mathbf{A}^{-1} \mathbf{B} \quad (2)$$

$$\mathbf{C}_{\mathcal{W}} = \mathbf{A}^{-1} \quad (3)$$

are frame invariant. The eigenvalues μ_1, μ_2, μ_3 of \mathbf{K}_V are the principal rotational stiffnesses, and the eigenvalues $\sigma_1, \sigma_2, \sigma_3$ of $\mathbf{C}_{\mathcal{W}}^{-1}$ are the principal translational stiffnesses.

The screw representation of a twist is a rotation about an axis followed by a translation parallel to the axis. The screw is usually described by the rotation axis, the net rotation magnitude M , with the independent translation specified as a pitch, h , that is the ratio of translational motion to rotational motion. For a twist (Murray et al. [7]) $h = \boldsymbol{\omega} \cdot \mathbf{v} / \|\boldsymbol{\omega}\|^2$, $M = \|\boldsymbol{\omega}\|$, and the axis of the screw is parallel to $\boldsymbol{\omega}$ passing through the point $\mathbf{q} = \boldsymbol{\omega} \times \mathbf{v} / \|\boldsymbol{\omega}\|^2$. A pure translation (where $\boldsymbol{\omega} = \mathbf{0}$) has $h = \infty$ and $M = \|\mathbf{v}\|$, with the screw axis parallel to \mathbf{v} passing through the origin. A unit twist has magnitude $M = 1$, in which case, for $\boldsymbol{\omega} \neq \mathbf{0}$, $h = \boldsymbol{\omega} \cdot \mathbf{v}$ and $\mathbf{q} = \boldsymbol{\omega} \times \mathbf{v}$. For a small screw motion with $M = \alpha$ and $\boldsymbol{\omega} \neq \mathbf{0}$, a point located at a distance ρ from the screw axis will be displaced by length

$$l \approx |\alpha| \sqrt{\rho^2 + (\boldsymbol{\omega} \cdot \mathbf{v})^2} \quad (4)$$

Equation 4 is the basis of the frame-invariant quality measure for compliant grasps described by Lin et al. [3]. Because the principal rotational and translational stiffnesses have different units, they cannot be directly compared to one another. One solution is to scale the principal rotational stiffnesses by an appropriate factor (see Lin et al. [3] for details) to yield the so-called equivalent stiffnesses, $\mu_{\text{eq},i}$:

$$\mu_{\text{eq},i} = \mu_i / (\rho_i^2 + (\boldsymbol{\omega}_i \cdot \mathbf{v}_i)^2) \quad i = 1, 2, 3 \quad (5)$$

where, μ_i is an eigenvalue of \mathbf{K}_V with an associated eigenvector $\boldsymbol{\omega}_i$, and ρ_i is the distance between the point of interest and the screw axis of the twist $[\mathbf{v}_i^T \ \boldsymbol{\omega}_i^T]^T$. The equivalent stiffnesses can be compared to the principal translational stiffnesses which leads to the stiffness quality measure $Q = \min(\mu_{\text{eq},1}, \mu_{\text{eq},2}, \mu_{\text{eq},3}, \sigma_1, \sigma_2, \sigma_3)$. Q characterizes the least constrained displacement of the mechanism. Therefore, maximizing the smallest rotational and translational stiffnesses will minimize the worst-case displacement of the mechanism.

3 Spatial Stiffness and Surface Registration

Our spatial-stiffness model of surface-based registration is parameterized by N surface points with locations $\{\mathbf{p}_i\}$ and unit normal vectors $\{\mathbf{n}_i\}$ for $i = 1, \dots, N$. Suppose

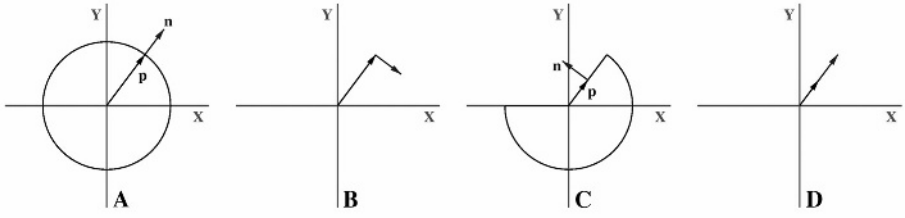


Fig. 1. Two examples of the dot product \mathbf{d}_{xy} . (A) A point \mathbf{p} on a circle in the xy plane and its associated surface normal \mathbf{n} . (B) The projection of \mathbf{p} onto the xy plane; \mathbf{n} is also projected but then rotated 90° in the plane. The dot product of the two vectors shown is $\mathbf{d}_{xy} = 0$; \mathbf{p} provides no rotational constraint about the z axis. (C) A point \mathbf{p} on an edge in the xy plane and its associated surface normal \mathbf{n} . (D) The projection of \mathbf{p} onto the xy plane; \mathbf{n} is also projected and then rotated 90° in the plane. The dot product of the two vectors shown is $\mathbf{d}_{xy} = \|\mathbf{p}\|$; \mathbf{p} provides good constraint about the z axis.

each point is displaced by a small translation $\delta = [t_x \ t_y \ t_z]^T$ and a small rotation $\mathbf{R} = \mathbf{R}_z(\omega_z)\mathbf{R}_y(\omega_y)\mathbf{R}_x(\omega_x)$. The locations \mathbf{q}_i of the displaced points are given by $\mathbf{q}_i = \mathbf{R}\mathbf{p}_i + \delta$. Because the displacement is small, we can take the region around each \mathbf{p}_i to be locally planar. The squared distance to the point on the surface nearest to \mathbf{q}_i is given by $((\mathbf{q}_i - \mathbf{p}_i) \cdot \mathbf{n}_i)^2$. Assuming a spring constant of unity, the potential energy U_i stored in each linear spring is $U_i = \frac{1}{2}((\mathbf{q}_i - \mathbf{p}_i) \cdot \mathbf{n}_i)^2$. It can be shown that the upper triangular part of the symmetric Hessian matrix \mathbf{H}_i of U_i evaluated at equilibrium is:

$$\begin{aligned} \mathbf{H}_i &= \mathbf{H}(U_i; \mathbf{v} = \boldsymbol{\omega} = \mathbf{0}) \\ &= \begin{bmatrix} n_{x_i}^2 & n_{x_i}n_{y_i} & n_{x_i}n_{z_i} & n_{x_i}\mathbf{d}_{yz_i} & -n_{x_i}\mathbf{d}_{xz_i} & n_{x_i}\mathbf{d}_{xy_i} \\ & n_{y_i}^2 & n_{y_i}n_{z_i} & n_{y_i}\mathbf{d}_{yz_i} & -n_{y_i}\mathbf{d}_{xz_i} & n_{y_i}\mathbf{d}_{xy_i} \\ & & n_{z_i}^2 & n_{z_i}\mathbf{d}_{yz_i} & -n_{z_i}\mathbf{d}_{xz_i} & n_{z_i}\mathbf{d}_{xy_i} \\ & & & \mathbf{d}_{yz_i}^2 & -\mathbf{d}_{xz_i}\mathbf{d}_{yz_i} & \mathbf{d}_{xy_i}\mathbf{d}_{yz_i} \\ & & & & \mathbf{d}_{xz_i}^2 & -\mathbf{d}_{xy_i}\mathbf{d}_{xz_i} \\ & & & & & \mathbf{d}_{xy_i}^2 \end{bmatrix} \quad (6) \end{aligned}$$

where $\mathbf{p}_i = [x_i \ y_i \ z_i]^T$, $\mathbf{n}_i = [n_{x_i} \ n_{y_i} \ n_{z_i}]^T$, $\mathbf{d}_{xy_i} = [x_i \ y_i] \cdot [n_{y_i} \ -n_{x_i}]$, $\mathbf{d}_{xz_i} = [x_i \ z_i] \cdot [n_{z_i} \ -n_{x_i}]$, and $\mathbf{d}_{yz_i} = [y_i \ z_i] \cdot [n_{z_i} \ -n_{y_i}]$.

The dot products, \mathbf{d}_{xy_i} , \mathbf{d}_{xz_i} , \mathbf{d}_{yz_i} , have important geometric interpretations. For example, \mathbf{d}_{xy_i} can be computed by projecting the vectors \mathbf{p}_i and \mathbf{n}_i onto the xy -plane; \mathbf{d}_{xy_i} is the dot product of the projected \mathbf{p}_i and a vector in the xy -plane that is perpendicular to the projected \mathbf{n}_i . An example of the dot products is illustrated in Figure 1. The dot products can also be interpreted as the x , y , and, z components of the cross product $\mathbf{p}_i \times \mathbf{n}_i$.

The spatial-stiffness matrix for surface registration is:

$$\mathbf{K} = \sum_{i=1}^N \mathbf{H}_i = \sum_{i=1}^N \begin{bmatrix} \mathbf{A}_i & \mathbf{B}_i \\ \mathbf{B}_i^T & \mathbf{D}_i \end{bmatrix} = \begin{bmatrix} \mathbf{A} & \mathbf{B} \\ \mathbf{B}^T & \mathbf{D} \end{bmatrix} \quad \text{where } \mathbf{A}_i = \begin{bmatrix} n_{x_i}^2 & n_{x_i}n_{y_i} & n_{x_i}n_{z_i} \\ n_{x_i}n_{y_i} & n_{y_i}^2 & n_{y_i}n_{z_i} \\ n_{x_i}n_{z_i} & n_{y_i}n_{z_i} & n_{z_i}^2 \end{bmatrix}$$

$$\mathbf{B}_i = \begin{bmatrix} n_{x_i} \mathbf{d}_{yz_i} & -n_{x_i} \mathbf{d}_{xz_i} & n_{x_i} \mathbf{d}_{xy_i} \\ n_{y_i} \mathbf{d}_{yz_i} & -n_{y_i} \mathbf{d}_{xz_i} & n_{y_i} \mathbf{d}_{xy_i} \\ n_{z_i} \mathbf{d}_{yz_i} & -n_{z_i} \mathbf{d}_{xz_i} & n_{z_i} \mathbf{d}_{xy_i} \end{bmatrix} \quad \mathbf{D}_i = \begin{bmatrix} \mathbf{d}_{yz_i}^2 & -\mathbf{d}_{xz_i} \mathbf{d}_{yz_i} & \mathbf{d}_{xy_i} \mathbf{d}_{yz_i} \\ -\mathbf{d}_{xz_i} \mathbf{d}_{yz_i} & \mathbf{d}_{xz_i}^2 & -\mathbf{d}_{xy_i} \mathbf{d}_{xz_i} \\ \mathbf{d}_{xy_i} \mathbf{d}_{yz_i} & -\mathbf{d}_{xy_i} \mathbf{d}_{xz_i} & \mathbf{d}_{xy_i}^2 \end{bmatrix} \quad (7)$$

In [5] we showed that aligning the centroid of the fiducial markers with the origin results in $\mathbf{B} = \mathbf{B}^T = [\mathbf{0}]$ which means that the rotational stiffnesses are decoupled from the translational stiffnesses. Although in general this cannot be done for surface registration or for stiffness matrices, Lončarić [4] showed that one can almost always choose a coordinate frame that maximally decouples rotational and translational aspects of stiffness, and that \mathbf{B} is diagonal in this frame.

In [5] we also showed that a single fiducial marker provided equal translational stiffness in all directions. Inspection of \mathbf{A}_i in Equation 7 shows that a single surface point only contributes to the translational stiffness in the $\pm \mathbf{n}_i$ direction. Thus, at least three surface points with linearly independent normal vectors are required to ensure that the principal translational stiffnesses (the eigenvalues of \mathbf{A}) are positive; the translation component of the registration transformation is well-constrained only if all of the translational stiffnesses are positive. Also note that the translational stiffnesses are independent of the locations of the surface points; only the orientations of the surface at the points are relevant. Given this observation it is easy to see how to stiffen a displacement with direction \mathbf{d} : simply choose a point where the surface has normal direction most closely aligned to $\pm \mathbf{d}$. Alternatively, apply a coordinate frame rotation so that \mathbf{d} is parallel to the z axis and find the point with normal vector that has the largest value of n_z^2 .

The analysis of the rotational stiffnesses is complicated by their being coupled to the translational stiffnesses. Let us focus on the matrix \mathbf{D} which relates torque to rotational displacement. There exists a coordinate frame rotation that diagonalizes \mathbf{D} because it is a symmetric matrix. The eigenvalues of this diagonal matrix are equal to the diagonal elements which are the squared dot products \mathbf{d}_{xy}^2 , \mathbf{d}_{xz}^2 , and \mathbf{d}_{yz}^2 . Suppose we want to stiffen the rotation about the z axis; this can be done by choosing a new point \mathbf{p}_i with normal vector \mathbf{n}_i so that $\mathbf{d}_{xy_i}^2$ is maximized. This leads to a heuristic for stiffening the rotation about the least-constrained rotational axis: apply a coordinate frame transformation so that the axis passes through the origin and is aligned with the z axis, then find the point with normal vector that maximizes $\mathbf{d}_{xy_i}^2$. This heuristic is not optimal because it ignores the coupling with the translational stiffnesses, but it may work in practice.

Simon [12] derived an expression for what he called a scatter matrix, Ψ ; this 6×6 matrix characterizes the sum of squared distance errors between a surface and a set of points from the surface displaced by a small rigid transformation. The expression for the scatter matrix is:

$$\Psi = \sum_{i=1}^N \begin{bmatrix} \mathbf{n}_i \\ \mathbf{p}_i \times \mathbf{n}_i \end{bmatrix} \begin{bmatrix} \mathbf{n}_i & \mathbf{p}_i \times \mathbf{n}_i \end{bmatrix} \quad (8)$$

Expanding Equation 8 and simplifying terms yields exactly the same expression as the stiffness matrix in Equation 7. An alternative and simpler derivation in the context of mechanism stiffness is already known (Huang and Schimmels [2]).

4 Strategies for Registration Point Selection

Simon [12] addressed the problem of choosing N points for registration by maximizing the noise amplification index (NAI)

$$\text{NAI} = \frac{\lambda_{min}^2}{\lambda_{max}} \quad (9)$$

where λ_{min} and λ_{max} are the smallest and largest eigenvalues of \mathbf{K} . The NAI was described by Nahvi and Hollerbach [8], and Simon [12] found that there were four important problems that must be addressed when using the NAI as a criterion for point selection.

The first problem is that the units of rotational and translational displacement are different. This means that the eigenvalues cannot be used unless they are scaled to compensate for the differing units. Simon [12] addressed this problem by translating the surface model so that its centroid was coincident with the origin, and isotropically scaling the model so that the average distance between the origin and the surface points was one. This solution is correct only for those scaled points that actually have unit distance from the origin. For long thin bones, this results in the NAI being less sensitive to rotations about the long axis of the bone.

The second problem is that \mathbf{K} and its eigenvalues are dependent on the coordinate frame; Simon [12] argued that the origin should be chosen to minimize λ_{min} , although he also noted that this did not result in large differences from simply centering the bone at the origin. The third problem is that the eigenvalues of \mathbf{K} , and thus the NAI, are sensitive to variations in the normal directions of the surface points; Simon [12] was forced to eliminate regions of high curvature from consideration for registration point selection. The fourth problem is that maximizing the NAI is a problem with combinatorial complexity; Simon [12] used hillclimbing and evolutionary techniques to solve this optimization problem. These algorithms are too time consuming to use online, and are not guaranteed to find the global maximum of the NAI.

Rusinkiewicz and Levoy [10] suggested choosing points so that the normal vector direction was uniformly sampled. This heuristic is generally inapplicable for typical surgical exposures. Recently, Gelfand et al. [1] suggested a technique called covariance sampling that uses an eigenanalysis of \mathbf{K} that is not frame invariant. Their stability measure is the condition number $\lambda_{max}/\lambda_{min}$.

Our approach to point sampling is to build a point set with a greedy algorithm that iteratively stiffens the least-constrained component found by the stiffness analysis of \mathbf{K} . Our algorithm can be described as follows:

- Manually choose an initial set of 6 registration points. We have found that the 3:2:1 fixturing concept (Shirinzadeh [11]) is a useful rule for choosing these 6 points.
- For $i = 7, 8, \dots, N$
 - Compute the stiffness matrix \mathbf{K} .
 - Compute the quality measure Q .
 - If Q corresponds to a translational stiffness
 - * Rotate the surface model so that least-constrained translational axis is parallel to the z axis.

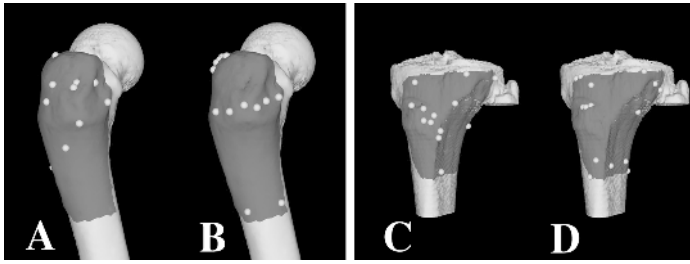


Fig. 2. Models, regions, and example point sets of size 15 used in our experiments. The proximal femur with (A) points chosen using the NAI and (B) our algorithm. The proximal tibia with (C) points chosen using the NAI and (D) our algorithm.

- * Choose \mathbf{p}_i with \mathbf{n}_i from the rotated model such that n_z^2 is maximized.
- * Undo the rotation applied to \mathbf{p}_i and \mathbf{n}_i .
- If Q corresponds to a rotational stiffness
 - * Translate and rotate the surface model so that least-constrained rotational axis passes through the origin and is parallel to the z axis.
 - * Choose \mathbf{p}_i with \mathbf{n}_i from the translated and rotated model such that $\mathbf{d}_{xyi}^2 = ([x_i \ y_i] \cdot [n_{yi} \ -n_{xi}])^2$ is maximized.
 - * Undo the transformation applied to \mathbf{p}_i and \mathbf{n}_i .

5 Experiments

We conducted experiments using our algorithm and by maximizing the NAI for point selection. We implemented the hillclimbing method described by Simon [12] for maximizing the NAI; we used the point set with the highest NAI after 10 restarts of the hillclimbing algorithm and allowed the algorithm to converge before each restart.

We used both methods to generate point sets of size $N = 6, 9, \dots, 30$. The running time of our algorithm is between two and three orders of magnitude smaller than the next ascent hillclimbing algorithm when run in Matlab on a SunBlade2000 workstation; all of the point sets for our experiments could be generated in approximately forty seconds when using the stiffness-based algorithm.

We used surface models of the proximal femur and the proximal tibia derived from CT scans of volunteers. For the femur, we chose points from the region surrounding the greater trochanter; this region was similar to the one we have used for several clinical cases of computer-assisted bone-tumor excisions. We used the location of a tumor from one of our clinical cases as the target; this point was located inside the neck of the femur. For the tibia, we chose points on the anterior and lateral surfaces consistent with the surgical exposure of a closing-wedge high tibial osteotomy. We used a point on the proximal medial side of the tibia as a target; this is a point on the hinge of osteotomy. The models, regions, and examples of point sets are shown in Figure 2.

To each point set we added noise drawn from the normal distribution with mean zero and standard deviation 0.5mm, and then applied a rotation of 1° about a random axis and

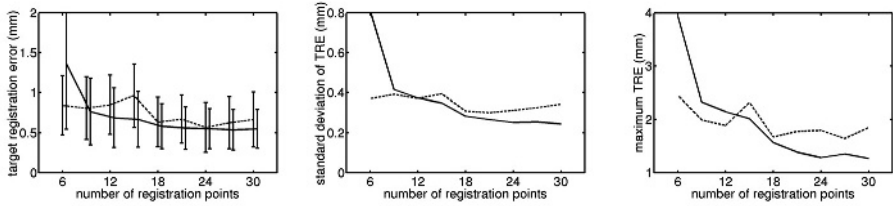


Fig. 3. Results for the proximal femur. Dashed lines are results using the NAI and solid lines are results for our algorithm. (Left) Mean TRE versus number of points; error bars are at ± 1 standard deviation. (Middle) Standard deviation versus number of points. (Right) Maximum TRE versus number of points.

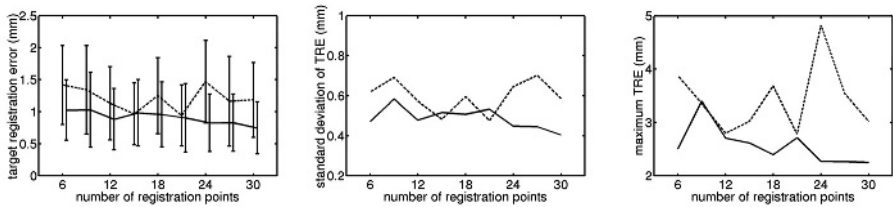


Fig. 4. Results for the proximal tibia. Dashed lines are results using the NAI and solid lines are results for our algorithm. (Left) Mean TRE versus number of points; error bars are at ± 1 standard deviation. (Middle) Standard deviation versus number of points. (Right) Maximum TRE versus number of points.

a translation of magnitude 0.5mm along a random direction; the point set was registered to the model using ICP and the TRE was computed. This process was repeated 500 times for each point set. The displacements we used were small because both our analysis and the NAI are based on the assumption of small displacements. The results are shown in Figures 3 and 4.

6 Discussion

Our heuristic algorithm, based on the stiffness quality measure, appears to perform as well as maximizing the NAI in terms of the mean TRE, and slightly better in terms of the maximum and variance of the TRE, for small displacements from the true registration; more tests, on a wider variety of surfaces, must be conducted before one can be confident in this conclusion. The behaviour of the TRE as a function of the number of registration points is much smoother for our algorithm than for the NAI-based algorithm, in part because the point set with N points is a superset of the one for $N - 1$ points when using our algorithm whereas the NAI-based algorithm always computes an entirely new point set. The most important advantage that our algorithm has over the NAI-based algorithm is that our algorithm is fast enough for online construction of point sets.

A limitation of our study is that the next-ascent hillclimbing algorithm is not guaranteed to converge to the global maximum of the NAI: the optimization of the NAI is a serious challenge for any algorithm that attempts to use it as a point selection criterion. Also, we have not shown that our point-selection scheme improves registration accuracy in practice, because our analysis of the matrix \mathbf{K} is limited to small displacements around the true registration. Simon [12] has provided empirical evidence that increasing the NAI by careful point selection tends to decrease the worst-case correspondence error. Perhaps the major limitation of our study is that we examine *model* registration points, whereas in practice a surgeon selects *anatomical* registration points; the critical, and unresolved, difference between the two is that the correspondence between model registration points and the model is known perfectly, while the correspondence between anatomical registration points and the model must be inferred. We postulate that resolving this difference will result in an algorithm for optimally analyzing the quality of a registration intraoperatively, and incidentally can suggest to a surgeon anatomical regions that might incrementally improve a registration for image-guided surgery.

Acknowledgments. This research was supported in part by the Institute for Robotics and Intelligent Systems, the Ontario Research and Development Challenge Fund, and the Natural Sciences and Engineering Research Council of Canada.

References

- [1] N. Gelfand, L. Ikemoto, S. Rusinkiewicz, and M. Levoy. Geometrically stable sampling for the icp algorithm. In *Proc 3DIM 2003*, 2003.
- [2] S. Huang and J. Schimmels. The bounds and realization of spatial stiffnesses achieved with simple springs connected in parallel. *IEEE Trans Robot Automat*, 14(3):466–475, 1998.
- [3] Q. Lin, J. Burdick, and E. Rimon. A stiffness-based quality measure for compliant grasps and fixtures. *IEEE Trans Robot Automat*, 16(6):675–688, Dec 2000.
- [4] J. Lončarić. Normal forms of stiffness and compliance matrices. *IEEE J Robot Automat*, RA-3(6):567–572, Dec 1987.
- [5] B. Ma and R. E. Ellis. A spatial-stiffness analysis of fiducial registration accuracy. In R. E. Ellis and T. M. Peters, editors, *MICCAI2003*, volume 1 of LNCS 2879, pages 359–366. Springer, November 2003.
- [6] B. Mishra and N. Silver. Some discussion of static gripping and its stability. *IEEE Trans Sys Man Cyber*, 19(4):783–796, Jul/Aug 1989.
- [7] R. M. Murray, Z. Li, and S. S. Sastry. *A Mathematical Introduction to Robotic Manipulation*. CRC Press, 1994.
- [8] A. Nahvi and J. M. Hollerbach. The noise amplification index for optimal pose selection in robot calibration. In *Proc Int Conf Robot and Automat*, 1996.
- [9] T. Patterson and H. Lipkin. Structure of robot compliance. *ASME J Mech Des*, 115(3): 576–580, Sep 1993.
- [10] S. Rusinkiewicz and M. Levoy. Efficient variants of the ICP algorithm. In *Proc 3DIM 2001*, pages 145–152, 2001.
- [11] B. Shirinzadeh. Issues in the design of the reconfigurable fixture modules for robotic assembly. *J Man Sys*, 12(1):1–14, 1993.
- [12] D. A. Simon. *Fast and Accurate Shape-Based Registration*. PhD thesis, Carnegie Mellon University, Pittsburgh, Pennsylvania, Dec 1996.